Fault zone signatures from ambient vibration measurements: a case study in the region of Visp (Valais, Switzerland)

Cyrill Baumann · Jan Burjánek · Clotaire Michel · Donat Fäh · Luis A. Dalguer

Abstract Investigations of tectonic features, such as faults, are important challenges for geologists and engineers. Although direct investigational methods, such as boreholes and trenches, have the potential to provide accurate data, these direct methods are usually expensive and time consuming, and give only punctual insights into subsurface structures. Geophysical methods, for example electric surveys and ground penetrating radar, are less expensive and faster to implement. However, these geophysical methods may be difficult or sometimes even impossible to apply in regions with rough topography or regions which are highly urbanized. In this study, we propose an easy-to-use and affordable method to detect fault zones based on ambient vibration observations. We apply this method in the region between Visp and Unterstalden (canton Valais, Switzerland) on a small fault branch, which has no explicit surface expression, and which is linked to a major fault zone, the Simplon Fault Zone. The assumption is that the fault of interest is surrounded by damage zone consisting of fractured rock, and that this results in lateral changes of both seismic velocity and attenuation. The objective was, first, to identify such lateral changes in the observed seismic wave-field, and second, to map any anomalies and combine them with the available geological information. In this way, we were able to follow the fault trace even without a clear surface expression of the fault. Our observations showed the existence of a signature in the power spectra of the seismic noise that may correspond to a damage zone. Such signature is observed along the trace of the expected fault.

Zusammenfassung Untersuchungen von tektonischen Einheiten, wie zum Beispiel Verwerfungen, stellen wichtige Herausforderungen für Geologen und Ingenieure dar. Obwohl direkte Untersuchungsmethoden, wie beispielsweise Bohrlöcher oder Grabungen das Potential in sich bergen, genaue Daten zu liefern, sind sie doch gewöhnlich sehr teuer, zeitintensiv und geben nur einen punktuellen Einblick ins Erdinnere. Geophysikalische Methoden wie elektrische Bodenuntersuchungen oder das Georadar sind zwar weniger teuer und einfacher in der Handhabung, diese Methoden sind aber oft nur sehr schwer oder teilweise gar unmöglich einzusetzen, vor allem im schweren Gelände oder in stark überbautem Gebiet. In dieser Studie präsentieren wir eine einfach anwendbare und vor allem kostengünstige Methode, um Verwerfungen mittels seismischer Bodenunruhe detektieren können. Wir wenden diese Technik in der Region zwischen Visp und Unterstalden an einer Nebenverwerfung der Simplon Linie an, die keinen expliziten Oberflächenausdruck aufweist. Dabei gehen wir von der Vermutung aus, dass die zu untersuchende Verwerfung das Gestein in seiner unmittelbaren Umgebung stark zerbrochen hat, was wiederum eine laterale Modifikation der seismischen Geschwindigkeit und Dämpfung zur Folge hätte. Das Ziel war es, eine solche

C. Baumann (✉) · J. Burjánek · C. Michel · D. Fäh · L. A. Dalguer
Swiss Seismological Service, ETH Zurich, Sonneggstrasse 5, 8092 Zurich, Switzerland
e-mail: cyrill.baumann@sed.ethz.ch

laterale Veränderung des beobachteten Wellenfeldes zu ermitteln, diese Anomalie zu kartieren und in einen geologischen Kontext zu setzen. Auf diese Weise konnten wir der Spur der Verwerfung auch ohne klaren Oberflächenausdruck folgen. Unsere Beobachtungen zeigen die Existenz einer Signatur im seismischen Spektrum des Hintergrundrauschens, die der gesuchten Verwerfung entsprechen könnte. Eine solche Signatur konnte über eine grössere Distanz hinweg identifiziert werden. Diese Beobachtungen, zusammen mit geomorphologischen und geologischen Hinweisen, stützen die Hypothese einer Verwerfung im entsprechenden Untersuchungsgebiet.

Résumé Les enquêtes sur les unités tectoniques, tels que des failles, sont des défis importants pour les géologues et les ingénieurs. Bien que les méthodes d'investigation directe, tels que les forages ou les tranchées aient le potentiel de fournir des données exactes, elles sont généralement très coûteuses, chronophages et ne donnent qu'un aperçu ponctuel des sous-sols. Les méthodes géophysiques telles que les sondages électriques ou les enquêtes géoradar sont moins chères et plus faciles à manipuler, mais ces méthodes sont souvent très difficiles, voir même impossibles à utiliser, surtout en régions urbanisées ou présentant un fort relief. Dans cette étude, nous proposons une méthode qui nous permet de détecter des failles au moyen du bruit de fond sismique. Nous utilisons cette technique dans la région entre Viège et Unterstalden sur une faille mineure, probablement associée au système extensif de la ligne de faille du Simplon, et qui n'a pas d'expression explicite en surface. Nous supposons que la faille à analyser est entourée de roches fracturées, ce qui aurait pour conséquence une modification latérale de la vitesse et de l'atténuation sismique. Le but est d'identifier une telle modification latérale du champ d'ondes observé, cartographier cette anomalie et de la replacer dans le contexte géologique relatif à la faille cherchée. Ainsi nous avons pu suivre la trace de la faille cherchée sans expression claire à la surface. Nos observations montrent l'existence d'une signature dans le spectre du bruit de fond sismique qui pourrait correspondre à la zone endomagée de la faille cherchée. Une telle signature a pu être identifiée le long de la faille supposée. Ces observations et les indices géomorphologiques soutiennent l'hypothèse d'une faille dans la région analysée.

1 Introduction

Seismicity of the Alps is considered as low to moderate (Giardini et al. 1999). However, the Valais area in the Swiss Alps shows the largest seismic hazard in Switzerland. During the past 500 years, the Valais region experienced five earthquakes with magnitudes estimated to have been around 6 (Fritsche 2008; Deichmann 2012). Earthquakes of this size occur with an average return period of about 100 years, the most recent one in 1946. The Valais presents rough topography, unstable and steep slopes, deep sediment-filled valleys and wide glacier- and snow-covered areas that potentially increase the risk level due to earthquake-induced phenomena such as strong site- and topographical effects, liquefaction, landslides and snow avalanches (Fäh et al. 2012). In addition, the design of buildings generally did not account for earthquakes until 2004, when the compliance with building codes started to be controlled, which makes the buildings stock vulnerable (Clotaire Michel, personal communication). Finally, important critical facilities, such as hydroelectric power plants and industry have been built in the Valais, making the region even more exposed to damaging earthquakes. The Tohoku earthquake of March 11, 2011, with a not-expected high moment magnitude of 9.0, has illustrated that the concatenation of individual events, in this case the earthquake effects, the tsunami and finally nuclear disaster, may have a tremendous impact on society. It is therefore essential, even in areas of low seismicity like Switzerland, to identify active faults and potential earthquake-induced effects and adequately mitigate the related risk.

In case of the Visp area, our study area, the recent seismicity rate is rather low and scattered so that the exact locations of active faults are unknown. However, the recently increased density of seismic stations in project COGEAR (COupled seismogenic GEohazards in Alpine Regions) will allow in the future to identify and map the active faults (Fäh et al. 2012). At present, it is not possible to link seismic events within anticipated fault zones in the Visp area. It is also difficult to identify the faults from observations of fault-trapped waves, as in the case of the San Andreas fault (e.g. Ben-Zion et al. 2003).

In this study, we propose an easy-to-use and affordable method to follow faults based on ambient vibration observations. We decided to test this technique in the area between Visp and Unterstalden (Fig. 1), since Marthaler (2003) mapped a minor fault in this region that seems to be associated with the extensional fault system known as the Rhone–Simplon Fault Zone, or, in the present area, simply the Simplon Fault Zone (SFZ). Moreover, in 1987, a local geologist, Charles-Louis Joris, observed traces interpreted as a neotectonic fault in the zone (Joris, personal communication), where Marthaler (2003) mapped the minor fault branch. Finally, a fault in the Eyholz road tunnel below the investigation site, which was discovered during construction (Norbert SA Geologie et al. 2006), is an additional indication of the presence of this fault which
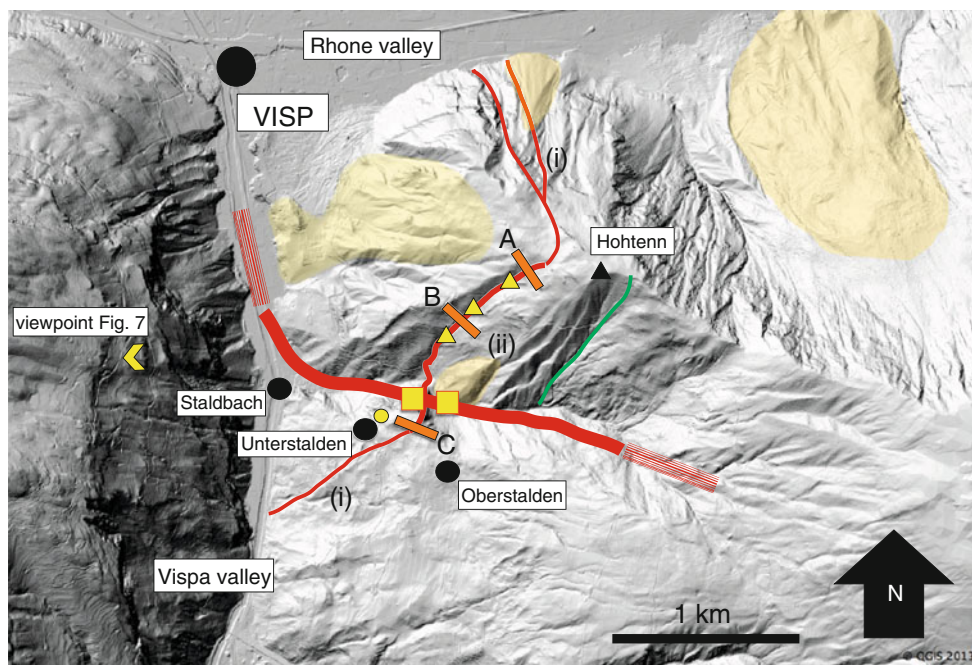
Fig. 1 LIDAR/Swisstopo DTM image of the survey investigation area, to the southeast of the town of Visp, in the Rhone valley at the north end of the Vispa valley (Valais, Switzerland). The *thick red line* marks a supposed trace of a segment of the Simplon Fault Zone (SFZ, Marthaler 2003), which follows the gorge called the Staldbachgraben, with a ca. E–W trend. The *thin red line*, trending approximately N–S represents the trace of the Hotée fault, which is probably also associated with the SFZ, as observed by Charles-Louis Joris, a local geologist (personal communication). *LIDAR* light detection and ranging, *DTM* digital terrain model. Along segments marked (*i*), the identification is less clear, whereas along segment (*ii*) was also mapped as a fault by Marthaler (2003), and a parallel-trending fault can be identified further to the east (*green line*). Triangles in *yellow* show the former outcrops, where Joris gathered indications for a neotectonic fault. The localization of the Hotée fault in the tunnel is labeled with a *yellow circle*. *Yellow boxes* show locations, where Campani could map the Simplon Line. *Orange rectangles* show locations, where we performed the ambient vibration measurements, Surveys *A*, *B* and *C*. *Yellow patches* show landslides and/or sagging areas (Joris, personal communication)

motivated our geophysical survey between Visp and Unterstalden.

Since the mapped fault branch (Marthaler 2003) has no explicit surface expression, and since the field observations of Mr. Joris (personal communication) are not visible anymore mainly due to the vegetation, we analyzed a Digital Terrain Model (DTM) based on a remote sensing method in order to get a rough idea of the trace of the potential fault and the required geometry of the array of seismic stations. Generally, faults are discontinuities along which fluid circulation and mechanical crunching have reduced rock strength (e.g. fault gouge and fault breccias). Because of this higher erodibility, faults are often followed by rivers, creeks, gullies, passes or gentle slope variations, allowing their detection by remote sensing (Sue et al. 2007). In particular, we analyzed light detection and ranging images (LIDAR, Swisstopo DTM, Fig. 1) to constrain geomorphologically the trace of the potential fault, since this image gathering method's abilities are to detect subtle topographic features in the land surface beneath the vegetation.

Earthquake ruptures and seismic radiation generate near-field stresses larger than the elastic limit, which results in an increasing crack density and therefore rock damage. The production of damage in the form of cracks is resisted by normal stress, and healing is enhanced by it. The evolution of rock damage over many earthquake cycles produces a flower-type fault zone structure, which exhibits significant shallow damage that decreases in amplitude and width with increasing depth (Finzi et al. 2010). The rock damage leads to a reduction of seismic velocity and increasing attenuation. This is consistent with detailed analysis of fault-zone trapped waves and other characteristics of rock damage (Ben-Zion et al. 2003).

Mapping of the subsurface structures using ambient vibration wave-field measurements is a common practice in geophysical prospecting (e.g. Fäh 1997; Bard 1998; Roten et al. 2006; Hellel et al. 2012). It has become increasingly attractive in a broad range of seismological disciplines at different scales, because of the relatively simple and efficient data acquisition (e.g. Fäh 1997). For example, the peak of the H/V spectral ratio is known to be correlated with sediment thickness and one can easily detect the lateral border between soft sediment and rock areas (e.g. Uebayashi 2003). Also, the change of the ambient vibration wave-field due to changes in the rock properties was

recently reported by Burjánek et al. (2010, 2012). In this study, we use the ambient vibration wave-field to detect zones of damaged rock. We do not assume any particular model for the wave propagation, we simply analyze the spatial pattern of the noise power spectra in the vicinity of the fault. Particularly, we setup dense linear arrays perpendicular to the anticipated fault trace and look for specific changes in the noise power spectra levels along the profile. We assume that the sources are at distances much larger than the array size. Generally, the main sources of ambient vibrations are the following (Bonnefoy-Claudet et al. 2006): for frequencies lower than 1 Hz, the source has usually a natural origin (e.g. tides, ocean waves), whereas for frequencies higher than 1 Hz the sources often have an anthropogenic origin (traffic, machines, industry, etc.). We expect that the ambient vibrations observed in the area of interest are mainly generated in the nearby industrial town of Visp, and are sufficiently far away from the study area to allow the method to be applicable.

The seismic surveys were performed during day and night, recording up to 3 h of ambient vibrations. The number of sensors was in average 10 and the spacing between them ranged from 9 to 115 m. Data acquisition was carried out with 5 s seismometers. All sensors were north oriented. The topography of the investigation area is fairly rough which made it difficult in some surveys to place the seismometers. We therefore decided to install seismometers, wherever possible, along conveniently located roads. The disadvantage was that we recorded noise from passing vehicles during the day as well as more rarely during the night. This additional noise source manifests itself in strong peaks in the seismic waveforms, especially during day measurements. Such short-duration disturbances of the signal were excluded from the spectral analysis by using an anti-trigger window selection. The objective was to keep the most stationary parts of the ambient vibrations, and to avoid the transients associated with specific sources (e.g. footsteps and close traffic). Windows were then processed individually to get individual spectra, which were finally averaged. The data were analyzed through spectral analysis, using a Fortran 90 library for multi-taper spectrum analysis (Prieto et al. 2009) to derive the power spectral density (PSD). The tapers are selected to optimally minimize broad-band bias due to the tendency for PSD to be influenced by strong peaks that spread into neighbouring frequency intervals of lower power (spectral leakage). In particular, the power spectral densities of each site were normalized by comparison with the PSD of a selected site (i.e. reference site). These so-called site-to-reference spectral ratios (SRSR) then represent frequency-dependent response functions with respect to the reference site. Although SRSR has been primarily used for earthquake recordings (Borcherdt 1970), it can be applied also to noise recordings, if it is assumed that the noise generating sources are far from the site (Roten et al. 2006; Burjánek et al. 2012). In this study, it is assumed that the distance of the study site from the town of Visp (ca. 2 km, Fig. 1) is sufficiently large to SRSR application.

2 Geological settings

The major geological feature in the investigation area is the Simplon Fault Zone (SFZ) (Fig. 2) (Mancktelow 1985, 1990; Merle et al. 1986; Mancel and Merle 1987; Steck 1990). This fault zone is a well-exposed low-angle detachment system developed in the Alps, resulting of orogen-parallel extension during the Oligocene–Miocene times (e.g. Mancktelow 1992). The SFZ is a wide zone of deformation, mainly marked by brittle deformation but with widespread ductile deformation within the footwall. The classic section of the SFZ is geographically situated between Visp and Domodossola (Italy), across the Simplon Pass, and corresponds to a major normal low-angle detachment system, with a general NW–SE strike and a low dip to the SW over a trace length of 30 km. This classic section is connected to the north with the Rhone Line, a major dextral strike-slip fault, which exhibits brittle deformation and runs along the Rhone valley (Fig. 2). The SFZ represents a major discontinuity that separates two main units, the upper Pennine nappes to the southwest from the lower Pennine nappes to the northeast (Milnes et al. 1981). The brittle deformation in the SFZ is confined to a narrow zone (<10 m) of cataclasites which is known as the Simplon Line (Fig. 2, see Mancktelow 1985; Mancel and Merle 1987; Steck and Hunziker 1994). At the village Simplon-Dorf, near the Simplon Pass, the Simplon Line dips 25°–30° towards SW.

In 1987, an active seismic survey was performed in the Western Alps as part of the project NFP20. The profile with the name West 3, which ran from Stalden to Zermatt (Heitzmann et al. 1991), was carried out west to the Simplon region. In this profile, (Marchant et al. 1993) interpreted the reflector emerging from the profile data as representing the Simplon detachment with a westward dip of about 30°. Debate centers on whether or not low-angle-detachment faults formed and/or slipped as "low-angle normal faults" (dip <30°), because standard fault mechanical theory (Anderson 1942) does not allow such orientations, and because earthquakes on such faults are rare (e.g. Jackson 1987). However, such structures are observed in the field and must be taken into considerations. The SFZ presents a telescoped crustal section of a single major low-angle fault system, initially dipping ≤30° and developed as an extensional feature during continued convergence (Campani et al. 2010a, b).

Fig. 2 Geological setting of the Simplon Fault Zone (SFZ) in the Central Alps, Switzerland. Geological map from Campani et al. (2010b) summarizing field observations of Campani et al. (2010a) and from published geological maps (Raron, Brig, Simplon, Domodossola) as well as field observations of Keller et al. (2005). The transition from strike-slip to normal fault occurs in the region of Visp. Hanging-wall is West and footwall East of the Simplon Line

Campani (2009) extensively studied the Simplon Line. She showed that the region between Visp and the villages of Unterstalden and Oberstalden, the present area of study, lies exactly where it becomes difficult to map the "Line" as one single discontinuity. It is clear that the fault zone is extending toward the Rhone valley, near Visp, but in the field it is difficult to follow (Campani, personal communication). Campani et al. (2010b) propose that the deformation is less localized in that region and that the single zone of brittle deformation splits into several branches. This is also supported by an identified jump in zircon fission track ages (Campani et al. 2010b), which is less localized than in classic sections, like the Zwischbergen valley or the region close to Simplon-Dorf. In those classic

sections, deformation from ductile to brittle behaviour is increasingly localized through time into a brittle detachment. There, one can see a clear separation between footwall (ductile shear zone) and hanging-wall (brittle deformation) by a fault gouge, which displays a sharp contact. Zircon fission track ages, which relate to the cooling of the rocks, show a sharp jump in the classic sections with younger ages in the footwall. However, in the section between Visp and Unterstalden, the overall jump in ages is similar but widely spread over a large distance. This simply implies that in the section near Unterstalden, the Simplon Line does not exhibit a sharp contact, but is rather a transition zone between the footwall and the hanging-wall which is strongly but more diffusely fractured.

Complex geological conditions were also evident during the construction of the tunnel Eyholz, which runs below the investigation area close to Unterstalden (Fig. 1). The tunnel crosses mainly calcareous mica schists, to a lesser extend hard and abrasive quartzites, prasinites and dolomites. These rock units are cut and displaced in parts by brittle faults. 1,500 m of the tunnel from Staldbach, below the zone of our surveys, the tunnel runs through a tectonically particularly highly fractured region, suggesting a connection to a major, regional, fault system, such as the Simplon Line and its continuation, the Rhone Line (Norbert SA Geologie et al. 2006). After 1,500 m from Staldbach, the geologic structure becomes less disturbed.

3 Results

3.1 Survey A

On the base of the LIDAR images, we considered it intuitively to perform Survey A in the upper extension of the couloir, just below the top of the hill Hohtenn (Fig. 1). Survey A was performed during the night and with 2 h of recordings. The measurements were conducted along a track across the field. No disturbances by traffic were observed. As a representative example, Fig. 3 shows normalized amplitude as a function of frequency (0.6–10 Hz) for the fault-normal component (perpendicular to the assumed fault) of Survey A. The amplitude was normalized with the mean amplitude of the array, which consists of 12 seismometers, at a frequency of 1 Hz. In this way we were able to identify the frequency range in which the differences in the site effects were most pronounced. This evaluation was performed for all surveys and for all components. The representative example in Fig. 3 clearly shows that for low frequencies, the signal is about the same for all receivers, but this is not the case in the frequency range between 2 and 7 Hz. In that fre-

quency band, the signals differ significantly. For higher frequencies (>7 Hz), the motions more or less agree again. The sharp peaks at 4.55 and 5.55 Hz, as well as above 7 Hz are due to machines, possibly coming from the Visp industrial zone. They have been also recognized on permanent seismic stations installed in the city of Visp. This kind of evaluation revealed also the frequencies of interest in Survey B (2–8 Hz) and Survey C (4–8 Hz). We then restricted the frequency band further, simply by trial-and-error, in order to see the anomaly as pronounced as possible. The spectral ratio with respect to the position along the profile of Survey A for a slightly shortened frequency band (2–4 Hz) is showing a clear spatial trend (Fig. 4). Spectral ratios allow identification of the differences between the stations' local site response. The general assumption is that the common (complex) signal of the stations in the array is due to sources of vibrations that are far enough to be considered the same at all points in the seismic survey area (Visp in Fig. 1). For each survey, we normalized the spectral ratio with the spectral ratio at the station, which exhibits the farthest distance from the main source Visp. In Survey A and B the reference stations were in both cases station 12, whereas in Survey C station 1 is the reference station. In Fig. 4, spectral ratio as a function of distance for fault normal, parallel and vertical component of Survey A is displayed. Seismometers are labelled black squares, station 1 is situated at a zero distance. All three, fault normal, parallel and vertical components show roughly the same pattern in the selected frequency range (2–4 Hz). Normal and parallel component exhibit a significant spectral ratio decay from station 5 to the spectral ratio minimum at station 9 along a zone with a length of about 112.5 m. Considering the vertical component, spectral ratio decreases significantly over a length of 153 m from station 5 to the spectral ratio minimum at station 10. Looking at the fault parallel component, the decrease from high amplitudes at stations 1–5 to low amplitudes at stations 9–12 is just about 12.4 % of the average value at stations 1–5, which clearly displays a change of physical properties along a narrow zone. The same applies to the fault normal (12.5 %) and vertical (16 %) component. The length along which we could detect the minimum value of the anomaly, in the normal and parallel component between station 9 and 10 and in the vertical component between station 10 and 11, was in all three components about 40 m. The upward trend or recovery of the reduced spectral ratios, particularly pronounced in the fault normal and parallel component, is an indication that the amplitude reduction cannot be simply explained by geometrical effects, i.e., by increasing distance from the potential major sources in the city of Visp.

Fig. 3 Ambient vibration survey data: normalized amplitude as a function of frequency (0.6–10 Hz) of Survey A (normal component, i.e. horizontal and perpendicular to the trace of the assumed fault). *Each line* represents a seismic station. At low frequencies (<2 Hz), the motion is about the same in all stations. For frequencies in the range between 2 and 7 Hz (*yellow box*), the signals are significantly different. For frequencies larger than 7 Hz, the signals are more or less consistent again
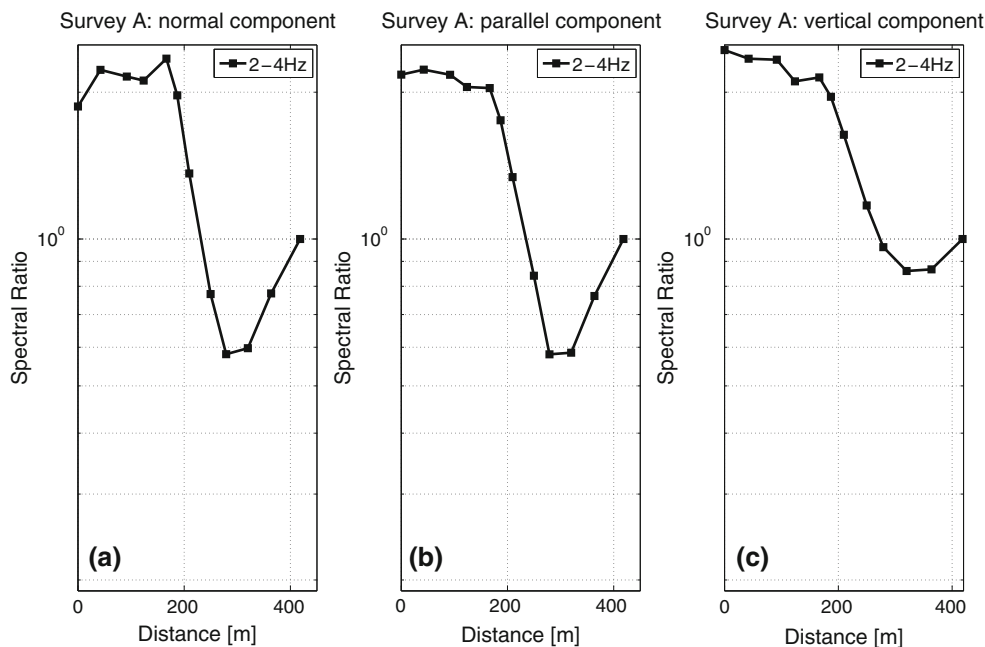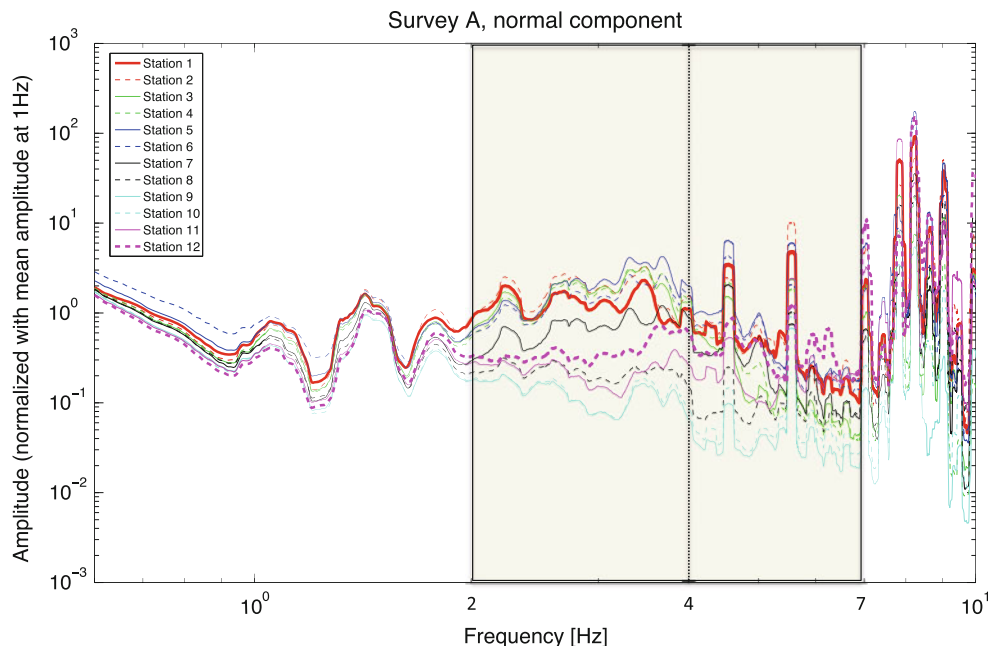

Fig. 4 Site-to-reference spectral ratio as a function of distance for ambient vibration Survey A (for location, see Fig. 1). The *black line* shows the frequency band, which comprises the values 2–4 Hz. Seismic sensors are marked as *black squares*. Station 1 is situated at zero distance, and has Swiss coordinates 635,442.012/126,064.684. Shown are: **a** fault-normal component; **b** fault-parallel component (i.e. horizontal, perpendicular to fault-normal); **c** vertical component.

Clearly visible is a decay of spectral ratio between station 5 and 9 in the normal and parallel component, and between stations 5 and 10 in the vertical component, and a subsequent recovery of spectral ratio in all three components, which marks the change of physical properties along the profile. In all three components, a spectral ratio minimum could be measured along a length of about 40 m

3.2 Survey B

Measurements of Survey B, which lies in the lower extension of the couloir, were performed along a street, crossing the potential fault. We set 12 stations and measured during daytime for around 1.5 h. There was no traffic on that road. The influence from the traffic on a main street, which was located several hundred meters away from the investigation site, was acceptable when compared to the stationary part of the signal. As in the data processing of Survey A, we
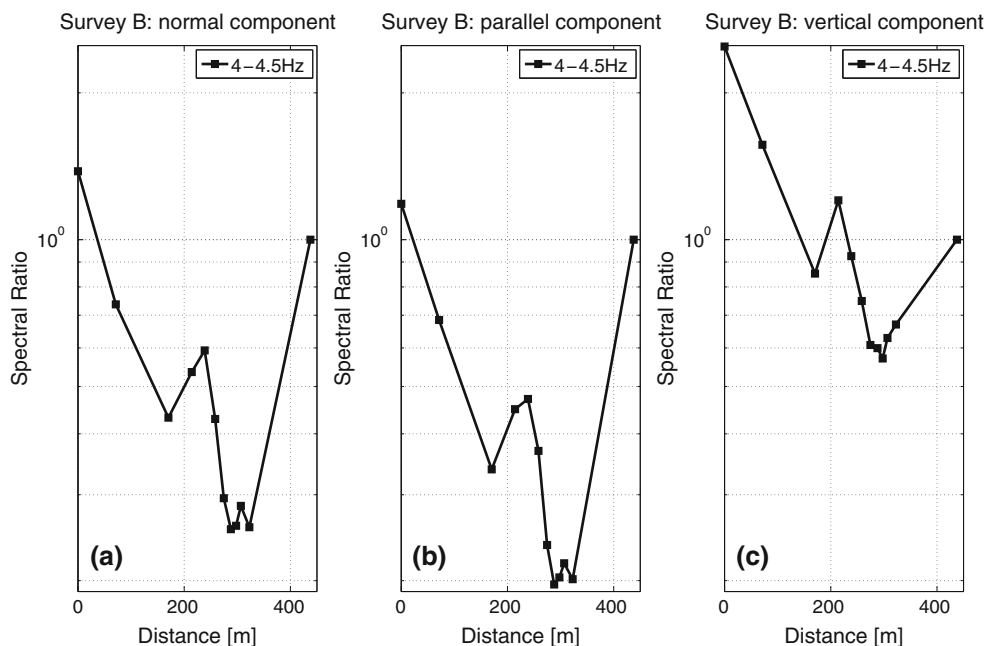
Fig. 5 Site-to-reference spectral ratio as a function of distance for ambient vibration Survey B (for location, see Fig. 1). The *black line* reflects the average over the frequency band, which comprises the values 4–4.5 Hz. Seismic sensors are marked as *black squares*. Station 1 is situated at zero distance, and has Swiss coordinates 634,921.2/125,679.7. Shown are: **a** fault-normal; **b** fault-parallel component (i.e. horizontal, perpendicular to fault-normal); **c** vertical component. Clearly visible is an amplitude reduction from station 1 to station 8 (normal and parallel component) and from station 1 to station 7 (vertical component). The zone with reduced spectral ratio potentially localizes a low velocity zone and can be measured along a distance of about 33 m

analyzed frequencies between 0.2 and 10 Hz in order to confine the frequency band such that we have the clearest signature of the anomaly, expressed in a reduction and subsequent increase of spectral ratio. In Survey B, the strongest effects were observed for the frequency range between 4 and 4.5 Hz. Figure 5 shows spectral ratio as a function of distance for frequencies between 4 and 4.5 Hz for the fault normal, parallel and vertical component. Normal and parallel components show a clear minimum in spectral ratios between station 8 and 11 along a distance of about 35 m. For the fault normal component, from station 1 to station 8, over a distance of 288 m, the spectral ratio decays to about 3.4 % of the spectral ratio at station 1 and does not change significantly up to station 11. From station 11–12, the amplitude increases to about 52 % of the value of the first station. The spectral ratio reduction is even more pronounced in the fault parallel component (decay to about 2.8 % of the value at station 1). The decay in the vertical component is about 6 % of the value at station 1. The recovery of the spectral ratio in the fault vertical component at station 11–12 is less distinct than in the normal and parallel component. It may be that the amplitude recovery continues beyond our seismic array. However, in all three components a weak to pronounced recovery of spectral ratio is observable. In all three components, the minimum of the ratios is measurable along a length of about 33 m and therefore comparable to the anomaly found in Survey A.

3.3 Survey C

Terrain analysis and the discovered fault in the tunnel (Norbert SA Geologie et al. 2006) brought us to perform Survey C north of Unterstalden (Fig. 1). The terrain at the location of Survey C was fairly difficult. Rough topography and dense vegetation impeded our measurements. Furthermore, the construction site of the tunnel Eyholz was now just below the site and closer than in the other arrays, which implies some potential sources of disturbances. Because of the rough terrain, we could only install 8 stations across the assumed fault and measured in the late morning for about 3 h. The total length of the survey line was 180 m, about half the length of Survey A and B. Figure 6 shows spectral ratios as a function of distance for frequencies in the range of 5.5–6.5 Hz. Spectral ratios of all components clearly show a downtrend from station 1–8. In the normal component, spectral ratio at station 8 is about 9 %, in the parallel component 23 % and in the vertical component 21 % of the value at station 1. Most likely, all stations in Survey C are affected by the noise in the tunnel, however, the downtrend in spectral ratio shows the change of physical properties over a distance of about 180 m. All 8 stations of Survey C are located at approximately the same distance from the assumed main source Visp and the tunnel, therefore an attenuation effect seems to be unlikely. Because of the lack of further stations to the east, we were

Fig. 6 Site-to-reference spectral ratio as a function of distance for ambient vibration Survey C. Seismic sensors are marked as *black squares*. Station 1 is situated at zero distance, and has Swiss coordinates 634,888.712/125,011.886. Shown are: **a** fault-normal component; **b** fault-parallel component (i.e. horizontal, perpendicular to fault-normal); **c** vertical component. All three components show a clear downtrend, or in another words: a change of physical properties
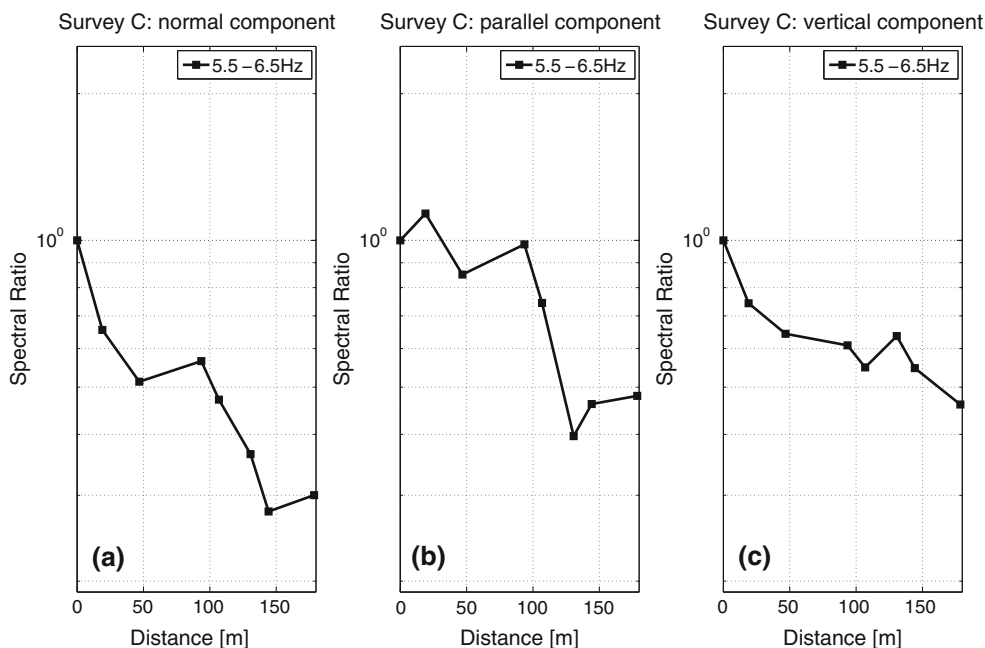
not able to detect a significant recovery of the spectral ratio in all three components.

In Survey A and B, a narrow zone in which spectral ratio is reduced could be identified in the frequency range of 2–4 Hz (Survey A) and 4–4.5 Hz (Survey B). In Survey A, the minimum width of that zone of strongest expected rock damage is about 40 m, in Survey B about 33 m. In Survey C, it was possible to detect a transition zone, in which physical properties are changing. The frequency range of interest was in that case 5.5–6.5 Hz.

4 Discussion

In summary, we were able to identify a most likely coherent anomaly along Survey A and B. We have also found an anomaly in Survey C, but its connection with the other two anomalies is not clear. Seismic anomalies found in Survey A, B and C represent the change of physical properties across the profiles. Their signatures in the seismic spectra display the transitions from sites with large to low amplitudes of the seismic waves in limited frequency bands. This cannot be explained by geometrical spreading, as a subsequent weak to significant recovery of the reduced amplitudes is observed in the spectral ratios of Survey A and B. The anomaly was best seen in the frequency range between 2 and 4 Hz in Survey A, between 4 and 4.5 Hz in Survey B and in the range of 5.5–6.5 Hz in Survey C. The main source of ambient vibrations in that frequency band is most likely the industrial zone in Visp. Local geological and geomorphological (Fig. 7) data seem

to support the results of these seismic surveys. The seismic anomaly, best revealed along Survey A and B, is in good agreement with the geological mapping of a fault branch in that area (Fig. 1, see Marthaler 2003), which seems associated with the Rhone–Simplon fault zone, although not parallel to the assumed trace of the Simplon Line in this area.

Certainly, the geometry of the surface topography can influence the seismic wave-field. However, it has much weaker influence with respect to changes of seismic velocities in the subsurface structure. For example, in the work of Burjánek et al. (2010), they observed no influence of the slope and topography shape on the estimated ambient vibration power spectral densities.

The anomaly found in Survey C is not as clear. There are several indications for faults in the vicinity of Survey C. For example Werenfels (1924) mapped a fault located a few meters away from Survey C between Unter- and Oberstalden. Furthermore, Campani and co-workers could map a branch of the Simplon Line along the road before Unterstalden (Fig. 1), where one can directly observe a fault gouge outcrop (Campani et al. 2010b). The observation near Unterstalden is very close to the location of Survey C. Observations were also made during the construction of the tunnel Eyholz, when a particularly pronounced fault was detected in the exploration tunnel with strongly folded, bulbous, graphite-bearing black schist. Its thickness in the exploratory tunnel is about 0.8–1 m. Survey C is situated close to this fault outcrop in the tunnel (Fig. 1) and may be the reason for the anomaly. However, the site conditions between Unterstalden and

Fig. 7 View from Zeneggen (see Fig. 1) looking eastwards along the deep trench called Staldbachgraben. *Red dashed line* shows part of the assumed surface trace of the Hotée fault (Joris, personal communication), which could have ruptured during the 1855 Visp earthquake (Fig. 1). *Red arrows* show where geomorphological indications for a separation between hanging-wall, on which Unterstalden is located, and footwall, on which Oberstalden is located, have been observed. This figure was taken from http://www.heidadorf.ch

Oberstalden, as well as the traffic in the area, made this region unfavourable for ambient vibration measurement and impacted measurement quality. Furthermore, the impact of a tunnel construction site close-by during the measurements is not entirely clear.

4.1 Possible link to the 1855 Visp Earthquake

On July 25, 1855, the strongest earthquake in Switzerland in the last 300 years struck the region of Visp with an estimated moment magnitude of 6.2 (Fäh et al. 2011). Visp, consisting of about 130 buildings at that time, was severely hit (Gisler et al. 2008; Fäh et al. 2012). People had to leave their buildings and live in tents for several weeks. Many of the houses built of stone masonry were heavily damaged, a few of them collapsed. Even wooden buildings suffered much harm. Besides Visp, significant damage was also reported for Stalden. The destruction was less than in Visp because of the large proportion of wooden buildings, but the stone masonry buildings suffered at least as much as those in Visp (Gisler et al. 2008). The earthquake triggered several secondary effects, such as terrain changes, soil liquefaction, landslides and rockfalls (Fritsche et al. 2006, 2012). Particularly affected by secondary effects were the regions between Visp and Stalden as well as the Matter valley.

The highest intensities of the main-shock were VIII (EMS-98, heavily damaging), and the aftershocks reached intensities of up to VII (damaging). Both the main-shock and the majority of the aftershocks affected primarily the villages in the valley between Visp and Stalden (Kozák et al. 2006), which may suggest the location of the fault. Furthermore, local observations that were reported indicate that the fault ruptured the surface. For instance, several observers reported large surface cracks even on bedrock sites (Fritsche 2008). The analysis of the damage field (Fritsche et al. 2006) revealed that the intensities in the west of the source (hanging-wall) were clearly higher than in the east (footwall), which is an indication for a normal N–S striking fault along the Vispa valley (Fig. 1). The hanging-wall and footwall of the Simplon fault presented in the study of Campani (2009) could explain the damage field of the 1855 Mw = 6.2 Visp earthquake (Fäh et al. 2011). A strike-slip to normal fault and normal fault regime in the region of Visp is however supported by Kastrup et al. (2004), who give insights into the predominant fault mechanism in the Alpine area. They analyzed systematically the state of stress of the central European Alps and northern Alpine foreland in Switzerland, based on focal mechanisms of 138 earthquakes with magnitudes between 1 and 5. The results of Kastrup et al. (2004) concerning the region of Visp were basically confirmed by Fäh et al. (2012).

4.2 Neotectonic evidences

Besides historical data, which suggest that the fault responsible for the 1855 event could be a normal fault striking north to south along the Vispa valley with hanging-wall in the west and footwall in the east (Fritsche 2008), there were also historical observations, which suggest that movement on the fault caused, at least in some parts, surface rupturing (Fritsche 2008). Since the 1855 earthquake is a young event, the sought fault would probably show neotectonic features in the ground surface. In 1987, in connection with the construction of the Eyholz tunnel between Staldbach and Grosshüs, a local geologist (Charles-Louis Joris, personal communication) carried out a geological mapping of the area between Visp and Unterstalden, where Survey A and B are in well agreement with a mapped fault (Marthaler 2003) probably associated with the Rhone–Simplon fault system. The observations refer to the morphologically marked side valley of the deep trench known as Staldbachgraben, between the mountain Hohtenn and the villages of Oberstalden and Unterstalden (Fig. 7). This suggested the presence of a NNE–SSW striking fault with a dip of ca. 60° to the WNW (Fig. 1). In the present study, this proposed fault was called Hotée fault, after a nearby hilltop. The Hotée fault can also be pursued south of the trench, between Oberstalden and Unterstalden, but less clearly defined (Fig. 7). In three different outcrops, he found macro-morphological indications for a neotectonic fault in that area. Those outcrops (Fig. 1) of the ductile rock type revealed young dislocations with clearly brittle fracture characteristics and offsets up to 15 cm. The fracture surfaces were neotectonic nature, yet edgy and only slightly weathered, suggesting a recent date of break in such a weathering and erodible rock. The observed fracture characteristics suggested brittle deformation at or very near to the contemporary surface (Joris, personal communication). These outcrops, located between Survey A and C (Fig. 1), are not visible anymore, because of the dense and thick regolith as well as the fact that the area is no long used for grazing or has been recently terraced for vineyards. An exhumation of the fault in the vineyard between Hohteen and Staldbachgraben by trenching or other structural measurements would surely reveal the about 25 years ago observed fault, and consequently the brittle fractures within a ductile, strongly fractured contact zone (Joris, personal communication).

It is likely that the fault which was discovered in the exploration tunnel during the construction of the Eyholz tunnel is the Hotée fault, since it has a similar strike (about NNW–SSE) and dips about 60° WSW (Norbert SA Geologie et al. 2006). Moreover, the Hotée fault, and the fault discovered in the exploration tunnel are characterized by the same material: black phyllites and shales. These observations could imply that this fault branch is a continuation of the Hotée fault and is therefore also of neotectonic nature. The seismic anomaly revealed particularly in Survey A and B, as well as in Survey C matches well with observations of both Joris (personal communication) and Marthaler (2003) and thus speaks for the detection of a real fault.

4.3 Estimation of fault size

Assuming that the Hotée fault was generated by the Visp 1855 earthquake, the question arises: what are the requirements in terms of fault size in order to generate a magnitude $M_w = 6.2$ earthquake such as that event? Wells and Coppersmith (1994) give an empirical relationship for estimating active fault dimensions, as follows:

$$A = 10^{(-2.87+0.82\,Mag)} \tag{1}$$

where A is the ruptured area and Mag the moment Magnitude. Equation (1) is valid for normal faulting and gives us a fault size of about 164 km². The simplified assumption of a square fault leads to a fault length of 12.8 km. Taking into account a dip of the Hotée fault, which is about 60° (Joris, personal communication; Norbert SA Geologie et al. 2006), the calculated depth extension of the fault seems to be reasonable, since such a fault would be entirely located within the seismogenic zone, which is limited in the Alps with a depth of about 20 km (Deichmann et al. 2000). Considering a fault length of about 12.8 km, the signatures observed in Survey A, B and C may correspond to a segment of about 1.1 km that belong to the causative fault of the 1855 Visp event. However, additional field investigations and seismic studies are required to test the hypothesis that the 1855 Visp earthquake was associated with movement on the Hotée fault.

5 Conclusions

Our results show a clear seismic signature in ambient vibration measurements along three profiles across a topographic feature situated between the villages Unterstalden and Oberstalden and the town of Visp, in the northern part of the Vispa valley. This signature is expressed in a reduction of the amplitude of the observed seismic waves in specific frequency bands between about 2 and 6 Hz. Our observations are supported by geomorphic indications revealed by LIDAR images as well as geological indications. The anomaly in Surveys A and B corresponds well to a fault mapped by Marthaler (2003), probably related to the Rhone–Simplon fault system, and denoted as Hotée fault (Joris, personal communication). Furthermore, close to Survey C, the Hotée fault could most

likely be identified in the tunnel construction site Eyholz. Because the rock in that region is tectonically highly deformed, a single delineation of the Simplon fault in that area is not possible, and several branches are identifiable. However, there are indications that the Hotée fault, which seems associated with the extensional system of the Simplon Line, and which was most likely identified in the tunnel Eyholz, could be the fault responsible for the 1855 Visp earthquake: (1) the reconstruction of the damage field of the Visp 1855 earthquake showed largest damage between Visp and Stalden, which may suggest the location of the fault; (2) observed phenomena (e.g. cracks in the ground, changes in springs) and the geological structure suggest that the causative fault might have reached the surface; (3) a normal fault striking along the N–S trending Vispa valley and dipping W was proposed by (Fritsche 2008; Wagner et al. 2000) and is supported by the macroseismic field of the Visp 1855 earthquake; (4) further geological observations depict the neotectonic nature of the Hotée fault (Joris, personal communication). We conjecture that the anomalies in Survey A, B and C are signatures in the power spectra of the ambient vibrations that correspond to a damage zone of the Hotée fault. When considering the indications given above, this fault could be part of the fault that ruptured on July 25, 1855, when the strongest earthquake in Switzerland in the last 300 years struck the region of Visp. The correlative conclusion to the event of 1855 is for now a hypothesis supported by the geological indications for a neotectonic fault in the considered area. However, in order to verify our hypothesis of a fault, further investigations are needed, whereby active seismics would be a possible approach. The increased density of seismic stations installed during project CO-GEAR (Fäh et al. 2012) will allow in future to detect the active faults in the investigation area.

References

Anderson, E. M. (1942). *The dynamics of faulting and dyke formation with application to Britain*. Edinburgh: Oliver and Boyd.

Bard, P.-Y. (1998). *Microtremor measurements: A tool for site effect estimation*: *Proceeding of the Second International Symposium on the Effects of Surface Geology on Seismic Motion, Yokohama, Japan* (vol. 3, pp. 1251–1279).

Ben-Zion, Y., Peng, Z., Okaya, D., Seeber, L., Armbruster, J. G., Ozer, N., et al. (2003). A shallow fault-zone structure illuminated by trapped waves in the Karadere–Duzce branch of the North Anatolian Fault, western Turkey. *Geophysical Journal International, 152*, 699–717.

Bonnefoy-Claudet, S., Cotton, F., & Bard, P.-Y. (2006). The nature of noise wavefield and its applications for site effects studies: A literature review. *Earth Science Reviews, 79*, 205–227.

Borcherdt, R. D. (1970). Effects of local geology on ground motion near San Francisco Bay. *Bulletin of the Seismological Society of America, 60*, 29–61.

Burjánek, J., Gassner-Stamm, G., Poggi, V., Moore, J. R., & Fäh, D. (2010). Ambient vibration analysis of an unstable mountain slope. *Geophysical Journal International, 180*, 820–828. doi:10. 1111/j.1365-246X.2009.04451.x.

Burjánek, J., Moore, J. R., Yugsi-Molina, F. X., & Fäh, D. (2012). Instrumental evidence of normal mode rock slope vibration. *Geophysical Journal International, 188*, 559–569. doi:10.1111/j. 1365-246X.2011.05272.x.

Campani, M. (2009). *Temporal and spatial evolution of a syn-orogenic extensional system: The Simplon Fault Zone (Central Alps)*. Ph.D. dissertation, ETH Zurich Nr. 18461, Zurich, Switzerland.

Campani, M., Herman, F., & Mancktelow, N. (2010a). Two- and three-dimensional thermal modeling of a low-angle detachment: Exhumation history of the Simplon Fault Zone, central Alps. *Journal of Geophysical Research Solid Earth, 115*, B10420. doi:10.1029/2009JB007036.

Campani, M., Mancktelow, N., Seward, D., Rolland, Y., Müller, W., & Guerra, I. (2010b). Geochronological evidence for continuous exhumation through the ductile-brittle transition along a crustal-scale low-angle normal fault: Simplon Fault Zone, central Alps. *Tectonics, 29*, TC3002. doi:10.1029/2009TC002582.

Deichmann, N. (2012). Earthquakes in Switzerland and surrounding regions 1996–2011. Sschweizerischer Erdbebendienst Jahresberichte. http://www.seismo.ethz.ch.

Deichmann, N., Baer, M., Braunmiller, J., Ballarin, D. D., Bay, F., Delouis, B., et al. (2000). Earthquakes in Switzerland and surrounding regions during 1999. *Eclogae Geologicae Helvetiae, 93*, 395–408.

Fäh, D. (1997). Microzonation of the city of Basel. *Journal of Seismology, 1*, 87–102.

Fäh, D., Giardini D., Kästli, P., Deichmann, N., Gisler, M., Schwarz-Zanetti, G., Alvarez-Rubio, S., Sellami, S., Edwards, B., Allmann, B., Bethmann, F., Wössner, J., Gassner-Stamm, G., Fritsche, S., & Eberhard, D. (2011). ECOS-09 Earthquake Catalogue of Switzerland Release 2011. Report and Database. Public catalogue, 17. 4. 2011. Swiss Seismological Service ETH Zurich, Report SED/RISK/R/001/20110417.

Fäh, D., Moore, J., Burjánek, J., Iosifescu, I., Dalguer, L., Dupray, F., Michel, C., Wössner, J., Villiger, A., Laue, J., Marschall, I., Gischig, V., Löw, S., Marin, A., Gassner, G., Alvarez, S., Balderer, W., Kästli, P., Giardini, D., Iosifescu, C., Hurni, L., Lestuzzi, P., Karbassi, A., Baumann, C., Geiger, A., Ferrari, A., Laloui, L., Clinton, J., & Deichmann, N. (2012). Coupled Seismogenic Geohazards in alpine Regions (COGEAR). *Bollettino di Geofisica Teorica ed Applicata, 53*, 485–508.

Finzi, Y., Hearn, E. H., Ben-Zion, Y., & Lyakhovski, V. (2010). Structural properties and deformation patterns of evolving strike-slip faults: Numerical simulations incorporating damage rheology. *Pure and Applied Geophysics, 166*, 1537–1573.

Fritsche, S. (2008). *Large historical earthquakes in Switzerland. Multidisciplinary Studies on Damage Fields and Site Effects*. Ph.D. dissertation, ETH Zurich Nr. 17710, Zurich, Switzerland.

Fritsche, S., Fäh, D., Gisler, M., & Giardini, D. (2006). Reconstructing the damage field of the 1855 earthquake in Switzerland: Historical investigations on a well-documented event. *Geophysical Journal International, 166*, 719–731.

Fritsche, S., Fäh, D., & Schwarz-Zanetti, G. (2012). Historical intensity VIII earthquakes along the Rhone valley (Valais, Switzerland): Primary and secondary effects. *Swiss Journal of Geosciences, 105*, 1–18.

Giardini, D., Grünthal, G., Shedlock, K. M., & Zhang, P. (1999). The GSHAP global seismic hazard map. *Annals of Geophysics, 42*, 1225–1230.

Gisler, M., Kozák, J., & Vaněk, J. (2008). The 1855 Visp (Switzerland) Earthquake: A milestone in macroseismic methodology? In Fréchet et al. (Eds.), *Historical seismology* (pp. 231–247). Netherlands: Springer.

Heitzmann, P., Frei, W., Lehner, P. & Valasek, P. (1991). Crustal indentation in the Alps—An overview of reflection seismic profiling in Switzerland. In R. Meissner et al. (Eds.) *Continental lithosphere: deep seismic reflections*, Geodyn. Ser., (Vol. 22, pp. 161–176), Washington, D. C.: AGU. doi:10.1029/GD022p0161.

Hellel, M., Oubaiche, E. H., Chatelain, J.-L., Machane, D., Bensalem, R., Guillier, B., et al. (2012). Basement mapping with single-station and array ambient vibration data: Delineating faults under Boumerdes City, Algeria. *Seismological Research Letters, 97*, 33–46.

Jackson, J. A. (1987). Active normal faulting and crustal extension. In M. P. Coward, J. F. Dewey, & P. L. Hancock, (Eds.), *Continental Extensional Tectonics. Geological Society Special Publication* (pp. 3–18). London: Blackwell Scientific Publication.

Kastrup, U., Zoback, M. L., Deichmann, N., Evans, K. F., Giardini, D., & Michael, A. J. (2004). Stress field variations in the Swiss Alps and the northern Alpine foreland derived from inversion of fault plane solutions. *Journal of Geophysical Research, 109*(B01402). doi:10.1029/2003JB002550.

Keller, L. M., Hess, M., Fügenschuh, B., & Schmid, S. M. (2005). Structural and metamorphic evolution of the Camughera-Moncucco, Antrona and Monte Rosa units southwest of the Simplon Line, Western Alps. *Eclogae Geologicae Helvetiae, 98*, 19–49.

Kozák, J., & Vaněk, J. (2006). The 1855 Visp (Switzerland) earthquake: Early attempts of earthquake intensity classification. *Studia Geophysica et Geodaetica, 50*, 147–160.

Mancel, P., & Merle, O. (1987). Kinematics of the northern part of the Simplon Line (Central Alps). *Tectonophysics, 135*, 265–275.

Mancktelow, N. (1985). The Simplon Line: A major displacement zone in the Western Lepontine Alps. *Eclogae Geologicae Helvetiae, 78*, 73–96.

Mancktelow, N. (1990). The Simplon Fault Zone. *Beitr. Geol. Karte Schweiz, NF 163*, p. 74.

Mancktelow, N. S. (1992). Neogene lateral extension during convergence in the Central Alps: Evidence from interrelated faulting and backfolding around the Simplonpass (Switzerland). *Tectonophysics, 215*, 295–317.

Marchant, R., Steck, A., Escher, A., Levato, L., Masson, H., Olivier, R., et al. (1993). An interpretation of the deep seismic lines from the Penninic Alps of Valais (Switzerland). *Bulletin de la Societe Geologique de France, 164*, 395–414.

Marthaler, M. (2003). Originalkarte Nr. 452 zu Blatt 1288 Raron (Südteil). *Geologischer Atlas der Schweiz 1:25'000*, Landesgeologie, swisstopo, Wabern.

Merle, O., Legal, P., & Mancel, P. (1986). Deformation and metamorphism in the Simplon region of the Central Alps. *Eclogae Geologicae Helvetiae, 79*, 705–718.

Milnes, A. G., Greller, M., & Müller, R. (1981). Sequence and style of major postnappe structures, Simplon-Pennie Alps. *Journal of Structural Geology, 3*, 411–420.

Norbert, S. A. Geologie et al, t. e. h., De Cérenville Géotechnique SA (2006). Tunnel Eyholz—Detailprojekt. Geologisch-Geotechnischer Bericht Beilage 3.1.

Prieto, G. A., Parker, R., & Vernon, F. L. (2009). A Fortran 90 library for multitaper spectrum analysis. *Computers and Geosciences, 35*, 1701–1710.

Roten, D., Cornou, C., Fäh, D., & Giardini, D. (2006). 2D resonances in Alpine valleys identified from ambient vibration wavefields. *Geophysical Journal International, 165*, 889–905.

Steck, A. (1990). A map of ductile shear zones of the Central Alps. *Eclogae Geologicae Helvetiae, 83*, 603–627.

Steck, A., & Hunziker, J. (1994). The Tertiary structural and thermal evolution of the Central Alps—compressional and extensional structures in an orogenic belt. *Tectonophysics, 238*, 229–254.

Sue, C., Delacou, B., Champagnac, J.-D., Allanic, C., Tricart, P., & Burkhard, M. (2007). Extensional neotectonics around the bend of the Western/Central Alps: An overview. *International Journal of Earthsciences, 96*, 1101–1129.

Uebayashi, H. (2003). Extrapolation of irregular subsurface structures using the horizontalto-vertical spectral ratio of long-period microtremors. *Bulletin of the Seismological Society of America, 93*, 570–582.

Wagner, J.-J., Frischknecht, C., Rosset, P., Sartori, M., Schindler, C., Beer, C., Mayer-Rosa, D., Rüttener, E., & Smit, P. (2000). Contribution au zonage sismique dans la vallée du Rhône, entre Sion et Brig, canton du Vailais, Suisse, projet SISVAL-IDNDR, *Landeshydrologie und geologie*, geological report no 25, 124 pp.

Wells, D. L., & Coppersmith, K. J. (1994). New empirical relationships among magnitude, rupture length, rupture width, rupture area, and surface displacement. *Bulletin of the Seismological Society of America, 84*, 974–1002.

Werenfels, A. (1924). Geologische Beschreibung der Lepontinischen Alpen. *Beiträge zur geologischen Karte der Schweiz 3. Teil*.